HHS Public Access

Author manuscript

ACS Appl Mater Interfaces. Author manuscript; available in PMC 2020 March 02.

Published in final edited form as:

ACS Appl Mater Interfaces. 2018 September 05; 10(35): 29357–29366. doi:10.1021/acsami.8b09819.

Nanofunctionalized Stent-Mediated Local Heat Treatment for the Suppression of Stent-Induced Tissue Hyperplasia

Jung-Hoon Park[†,‡,§,∇], **Wooram Park**[§,ǁ,∇], **Soojeong Cho**[§], **Kun Yung Kim**[†], **Jiaywei Tsauo**[†], **Sung Hwan Yoon**[†], **Woo Chan Son**[⊥], **Dong-Hyun Kim**[*,§,#], **Ho-Young Song**[*,†]

[†]Departments of Radiology and Research Institute of Radiology, Asan Medical Center, University of Ulsan College of Medicine, 88 Olymic-ro 43-gil, Songpa-gu, Seoul 05505, Republic of Korea

[‡]Department of Biomedical Engineering Research Center, Asan Medical Center, University of Ulsan College of Medicine, 88 Olymic-ro 43-gil, Songpa-gu, Seoul 05505, Republic of Korea

[⊥]Department of Pathology, Asan Medical Center, University of Ulsan College of Medicine, 88 Olymic-ro 43-gil, Songpa-gu, Seoul 05505, Republic of Korea

[§]Department of Radiology, Feinberg School of Medicine, Northwestern University, Chicago, Illinois 60611, United States

[ǁ]Department of Biomedical Science, College of Life Sciences, CHA University, 335 Pangyo-ro, Bundang-gu, Seongnam, Gyeonggi 13488, Republic of Korea

[#]Robert H. Lurie Comprehensive Cancer Center, Chicago, Illinois 60611, United States

Abstract

Current therapeutic strategies are insufficient for suppressing stent-induced restenosis. Here, branched gold nanoparticles (BGNP)-coated self-expandable metallic stents (SEMSs) were developed for a local heat-induced suppression of stent-related tissue hyperplasia. Our polydopamine (PDA) coating on SEMS allowed BGNP crystal growth on the surface of SEMSs. The prepared BGNP-coated SEMS showed effective local heating under near-infrared laser irradiation. The effectiveness of BGNP-coated SEMSs for suppressing stent-related tissue hyperplasia was demonstrated in a rat esophageal model ($n = 52$). BGNP-coated SEMS placement under fluoroscopic guidance was technically successful in all rats. The placed BGNP-coated SEMS in rat esophagus achieved three different local heat dose ranges (50, 65, and 80 °C) under fluoroscopic image-guided local irradiation. Follow-up endoscopic examination readily monitored the local heating and observed significantly decreased tissue hyperplasia at 4 weeks of local heat treatments (50 and 65 °C). Finally, Western blot, histology, immunohistochemistry (HSP70, αSMA, and TUNEL), and immunofluorescence (Ki67 and BrdU) analyses along with the

[*]**Corresponding Authors:** dhkim@northwestern.edu, hysong@amc.seoul.kr.

[∇]Author Contributions

J.-H.P. and W.P. contributed equally to this work and are cofirst authors.

Supporting Information

The Supporting Information is available free of charge on the ACS Publications website at DOI: 10.1021/acsami.8b09819. Measurement of temperature change of BGNP-coated SEMS by repeated laser irradiation; immunohistochemical analysis for re-epithelialization after BGNP-coated SEMS local heating (PDF)

The authors declare no competing financial interest.

statistical analysis confirmed that optimized BGNP-coated SEMS-mediated local heat treatments inducing the expression of anti-inflammatory HSP70 effectively suppresses tissue hyperplasia after stent placement in the esophagus. Our local heating with nanofunctionalized stents represents a promising new approach for suppressing stent-related tissue hyperplasia.

Graphical Abstract

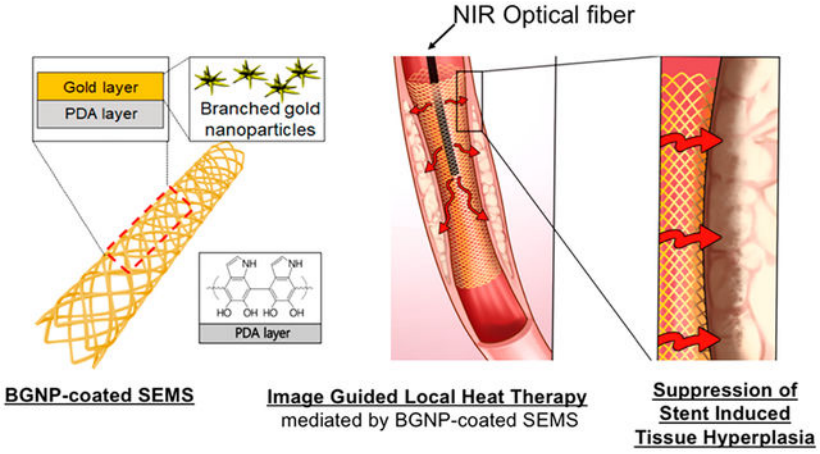

Keywords

self-expandable metallic stent; tissue hyperplasia; local heat therapy; gold nanoparticles; nanofunctionalization

INTRODUCTION

Placement of a self-expandable metallic stent (SEMS) has been used to treat unresectable esophageal malignancy or benign esophageal strictures refractory to repeated balloon dilations.[1–3] However, the use of SEMSs is greatly limited by recurrent stent obstructions due to tissue hyperplasia within or above and below the SEMSs.[2–5] This tissue hyperplasia caused by the SEMS occurs as a proliferative response resulting from mechanical stent-induced injury on the esophageal wall.[2,6] Antiproliferative drug-eluting SEMSs (e.g., transforming growth factor beta inhibitor or paclitaxel), biodegradable stents, and alternative stent designs have been investigated to prevent or decrease tissue hyperplasia; however, the current therapeutic strategies remain insufficient for clinical trial.[6–10]

Local heat treatment in the thermoregulatory biosystem offers extensive opportunities to manipulate biological events such as cell proliferation, cellular signaling, immune reaction, protein denaturation, and so on.[11] Representatively, controlled local heat treatments have been introduced to induce irreversible cell injury and immune stimulation.[11–13] Radio waves, microwaves, ultrasound waves, and other forms of energy sources have been used for the heat treatments.[14,15] Recently, various nanoparticles including gold nanoparticles (GNPs) and magnetic nanoparticles have also been studied extensively for thermal treatments with high efficiency and accuracy.[16–19] In addition to those applications, a local heating may provide an opportunity to suppress tissue hyperplasia following stent

placement. A mild local heating has been effective to reduce collagen accumulation, increase cell apoptosis, alter cell metabolism, and activate a family of heat shock proteins (HSPs).[12,13] Thus, heat treatment using lasers or hot water was tested for a potential in decreasing in-stent restenosis[13,20] and inhibiting tissue hyperplasia.[12] However, nonspecific or excessive heating might result in normal tissues being damaged and sometimes rather enhance tissue hyperplasia after the stent placement. Herein, we hypothesized that near-infrared (NIR)-absorbing GNPs-coated SEMS-mediated photothermal (PT) local heat treatment could effectively prevent the tissue hyperplasia after SEMS placement. For the efficient in vivo local heating of SEMSs, branched gold nanoparticles (BGNPs),[21,22] which have shown effective photothermal heating properties, were considered for the functionalization of SEMS. To fabricate the BGNP-coated SEMSs, the surface of nitinol SEMS were modified with polydopamine (PDA). Then, BGNP crystal growth in sodium deoxycholate solution[21] was induced on the PDA surface on SEMS. The formed BGNPs on the surface of SEMSs were characterized, and BGNP-mediated NIR PT heating of BGNP-coated SEMSs was investigated for potential local heat-induced suppression of tissue hyperplasia applications. Finally, our in vivo rat esophageal model studies including BGNP-coated SEMS placement and image-guided local heat-treatment with interventional approaches, follow-up endoscopic examination, Western blot and pathological analyses, along with the statistical analysis demonstrated that BGNP-coated SEMS-mediated local heating suppresses stent-related tissue hyperplasia.

RESULTS AND DISCUSSION

Characterization of BGNP-Coated SEMS.

BGNP-coated SEMSs were successfully fabricated using a two-step synthesis process (Figure 1a). The bare nitinol SEMS was first coated with PDA on the surface. Then, BGNPs were successfully grown on the surface of SEMS following a modified procedure outlined in our previous report.[21] Scanning electron microscopy (SEM) images showed that the anionic BGNPs were uniformly coated through electrostatic interactions by the PDA-mediated cationic polymer coating layer. Elemental analysis (Figure 1b–d) revealed that a signal for gold (red) was significantly increased in the BGNP-coated SEMS. Strong nickel (blue) and titanium (green) signals were also detected because of the nitinol wires of the SEMS. The PDA coating on the SEMS resulted in an enhanced carbon (pink) signal compared to the control SEMS. The coating layer was approximately 7 μm thick according to the SEM images (Figure 1e). When the surface of BGNP-coated SEMS was analyzed by SEM, GNPs with a branched structure were observed (Figure 1f). Additionally, to confirm the successful growth of BGNPs on the surface of BGNP-coated SEMS, BGNP was extracted from the BGNP-coated SEMS and analyzed by SEM and transmission electron microscopy (TEM). As shown in Figure 1f,g, GNPs in the form of branches were observed, which is similar to our previous report.[21] The coated metal nanoparticles on the SEMSs were also confirmed with extinction spectra showing a strong absorption band at around 720 nm in the near-infrared region (Figure 1h). Although esophageal stents with similar gold nanostructures have recently been reported,[23] the stent can be manufactured using a complex lithography process and thus has limitations in practical clinical use. In this regard, it is significant that

we successfully introduced branched gold nanostructures into metal SEMS using a simple chemical process.

Characterization of NIR Photothermal Heating of BGNP-Coated SEMS.

Strong NIR absorption induced by the formed BGNP on the stent directly generated significant heating upon NIR 808 nm irradiation. The temperature of BGNP-coated SEMS rapidly reached a relatively high steady-state temperature compared to the control and PDA-coated SEMSs in 50 s after NIR laser irradiation and rapidly cooled after cessation of irradiation. Under a fixed power of NIR laser 1.27 W/cm^2, the mean steady-state temperatures (°C, ± SD) of the control, PDA-coated, and BGNP-coated SEMSs were 40.05 ± 0.48, 43.25 ± 0.25, and 50.42 ± 0.41, respectively (Figure 2a). When the laser energy level changed from 0.64–2.55 W/cm^2, the mean steady-state surface temperatures (°C, ± SD) of BGNP-coated SEMSs were each 35.66 ± 0.42 at 0.64 W/cm^2, 50.27 ± 0.64 at 1.27 W/cm^2, 65.38 ± 0.89 at 1.91 W/cm^2, and 81.07 ± 0.65 at 2.55 W/cm^2 (Figure 2b). These results indicate that BGNP-coated SEMSs generate excellent local heat energy with NIR irradiation, and the local heating properties can be easily controlled by simply adjusting NIR irradiation power.[21,22] Additionally, to confirm the stability of heat generation of the stent by light irradiation, the NIR laser light was irradiated to the BGNP-coated SEMS five times and the surface temperature of the stent was measured. As shown in Figure S1 (Supporting Information), when the NIR laser (intensity, 1.91 W/cm^2) was turned on, the temperature rose rapidly to 65 °C, and the temperature dropped rapidly when the light irradiation was stopped. These results were no different during the five replicates. This result implies that the BGNP-coated SEMS has excellent optical stability. Prior to the in vivo studies, our BGNP-coated SEMS-mediated local heating was further tested in the ex vivo rat esophagus. As shown in Figure 2c–f, BGNP-coated SEMS and NIR laser (1.91 W/cm^2) irradiation in the rat esophagus achieved a specific local heating reaching the maximum of 64.26 ± 0.42 °C at the proximal end of the stent and 61.87 ± 0.37 °C at the distal end of the stent (Figure 2g). The ex vivo results were similar to the measured temperature of surface of BGNP-coated SEMS.

In Vivo Animal Groups, Stent Placement, Local Heating, and Endoscopic Findings.

For this study, 52 male Sprague–Dawley rats (Orient Bio, Seongnam, Korea) weighing 300–350 g were used. Rats underwent BGNP-coated SEMS placement and were randomly divided into four groups using computer-generated random numbers as follows: group A (n = 13) received no heat treatment (control) and groups B (n = 13), C (n = 13), and D (n = 13) received a single fraction of BGNP-coated SEMS-mediated local heating (50, 65, and 80 °C, respectively) after the stent placement, respectively (Figure 3a). The number of animals was calculated according to a previously published study.[6] Ten rats from each group were euthanized 4 weeks after stent placement for histopathological examinations. In our previous study,[24] we observed changes in tissue after 4 weeks of stent transplantation, so the experiments were conducted under the same conditions for comparison. Three rats from each group were used for Western blot analysis immediately after local heating. Stent placement under fluoroscopic guidance was technically successful in all rats (n = 52) (Figure 3b). However, 3 of 52 (5.7%) rats died after stent placement because of hemorrhage caused by the barbs of the stent (one each in groups A, C, and D) 1–3 days after stent placement.

BGNP-coated SEMSs migrated into the stomach in five rats (one each in groups A, B, and D and two in group C) within 10 days after stent placement. The remaining 44 (84.6%) rats survived until the end of the study without stent-related complications.

For groups B, C, and D, BGNP-coated SEMS-mediated local heating was performed at 10 days after the stent placement in all rats. Group A, the control group, was treated with BGNP-coated SEMS placement only without heating. For BGNP-coated SEMS-mediated local heat treatment in groups B, C, and D, an optical fiber loaded in a 6-Fr radiopaque sheath was introduced through the mouth into the midportion of the stented esophageal lumen under fluoroscopic guidance (Figure 3c). NIR light (1.27, 1.91, and 2.55 W/cm^2 for groups B, C, and D, respectively) from the optical fiber was locally irradiated in the stented esophageal lumen for 60 s. Subsequent endoscopic examination right after the NIR heating showed a white-colored deformed esophageal mucosa adjacent to the stent in groups B, C, and D (Figure 3d). Finally, follow-up in vivo endoscopic images at 4 weeks after the stent placement showed a widely patent smooth esophageal lumen with apparently suppressed tissue hyperplasia in groups B (Figure 3f), C, and D compared to the severe tissue hyperplasia through the wire mesh in group A (Figure 3e).

In Vivo Suppression of Stent-Induced Tissue Hyperplasia Using Nanofunctionalized Stent-Mediated Photothermal Local Heating.

Surgical exploration of the esophagus and stomach was followed by gross examination to determine possible esophageal changes after stent placement or stent-mediated local heat treatment. The stented esophageal segment of each group was sectioned transversely at the proximal, middle, and distal regions for histology, immunohistochemistry (IHC), and immunofluorescence (IF) analysis. Analysis of hematoxylin and eosin (H&E) and Masson's Trichrome (MT) stained tissues clearly demonstrated the significant decrease of excessive tissues including granulation tissues, epithelial layers, collagen deposition, connective tissue, and submucosal fibrosis on the stented esophageal strictures in groups B, C, and D compared with group A (Figure 4a,b). Specifically, granulation tissue formation after stent placement in group A was significantly diminished after the local heat treatment with BGNP-coated SEMS (groups B, C, and D) (Figure 4c). Although heating group D at 80 °C was less effective in terms of suppressing excessive tissues than groups B (50 °C) and C (65 °C), tissue hyperplasia was significantly less in group D than in group A (Figure 4c).

Although SEMSs are gaining popularity in medicine because of their ease of placement and lack of invasiveness compared to other surgical techniques, a well-known complication of stent placement in patients is the eventual formation of tissue hyperplasia resulting in restenosis.[3–5] Shearing forces created by differential motion of the stent relative to the esophagus contribute to the constant stimulation of the esophageal wall, leading to wounds and inflammatory reaction and resulting in tissue hyperplasia. The chronic inflammation induced by stents placed in the esophagus may predispose to tissue proliferation.[25] Given the inflammatory reaction in tissue hyperplasia, anti-inflammatory immunosuppressive treatments would be a more radical approach to reduce the risk of tissue hyperplasia. Our local heat treatment inducing various HSPs might result in potent immune suppression along with an inhibitory action on smooth muscle and endothelial cell proliferation. It is well-

reported that HSP70 among various HSPs is capable of exerting anti-inflammatory effects by repairing denatured proteins, dissociating initial loose protein aggregates, and ensuring correct folding and translocation of proteins.[25,26] To investigate the HSP70 expression by our BGNP-coated SEMS-mediated local heating, 3 rats in each group were euthanized at 3 days after the stent-mediated local heating, and the stent-containing esophageal segments were harvested for Western blot analysis of HSP70. As expected, the relative HSP70 expression significantly increased in groups B, C, and D compared to group A or the normal value of the rat esophagus (all variables; $p < 0.001$) (Figure 5a,b). The HSP70 expression gradually increased in a heating dose-dependent manner (Figure 5a,b). This demonstrated HSP70 expression after our local heating was further confirmed in IHC analysis of each group at 4 weeks. Significantly higher HSP70 expression was still measured in groups B, C, and D compared with group A (all variables; $p < 0.001$) (Figure 5c,d). In turn, the enhanced HSP70 expression of groups B and C resulted in effective suppression of stent-related tissue hyperplasia with lower level of inflammatory cell infiltration than in groups A and D (all variables; $p < 0.001$) (Figure 4c). However, an excessive heating (80 °C) in group D was not as suppressive as groups B (50 °C) and C (65 °C). TUNEL stained tissues of each group indicated that an intense heat treatment (i.e., 80 °C) caused irreversible damage to extra normal tissues (Figure 5c) and induced massive cell killing leading to additional inflammatory reactions (Figure 4c). Subsequently, during the proliferative phase, formation of the epithelium occurs to cover the wound surface with concomitant growth of granulation tissue.[26] Relatively high temperatures (80 °C) may promote more re-epithelialization after BGNP-coated SEMS local heating, as demonstrated by significantly higher alpha-smooth muscle actin (αSMA)-positive-deposition in group D than groups B and C (all variables; $p < 0.05$) (Figure S2, Supporting Information).

Lastly, 5-bromo-2-deoxyuridine (BrdU) and K_i-67, which are principle markers for mitotic cells, were investigated to observe the status of cell proliferation in the regions of the stents (all groups). While the anti-inflammatory HSP70 expression of group B and C was significantly increased in the esophageal mucosa, the markers of cellular proliferation were significantly decreased after BGNP-coated SEMS-mediated local heating of groups of B and C compared to groups of A (Figure 6). Taking all results together, our findings suggest that moderate BGNP-coated SEMS-mediated local heat treatments (50 and 65 °C) of groups B and C suppress tissue hyperplasia and minimize tissue remodeling after the stent placement. Further studies are warranted to refine the optimal temperature ranges and timing for local heating to suppress stent-induced tissue hyperplasia.

CONCLUSION

Minimally invasive management of esophageal strictures using stent technology is currently limited by the development of tissue hyperplasia adjacent to the SEMS. The progressive tissue ingrowth through the wire filaments leads to recurrent stent obstructions.[27] Severe tissue hyperplasia often causes difficulties in nonsurgical removal of the metallic stents.[28] In this study, we were able to successfully coat SEMSs with BGNPs and the BGNP-coated SEMS generated significant heat ex vivo and in vivo when irradiated with a NIR laser. In the in vivo study, an optical fiber for NIR laser irradiation was easily delivered through the working channel of interventional endoscopy to the region of BGNP-coated SEMS

placement. Under fluoroscopy and endoscopic visualization, a BGNP-coated SEMS-mediated local PT therapy could be applied to a region of interest. This therapeutic strategy can also be used for tumor ingrowth and/or overgrowth through the uncovered portion or disrupted covering membrane after stent placement in patients with esophageal cancer. Three different temperatures (50, 65, and 80 °C) were used to evaluate the dose-range effect. Our results in Western blot, histology, IHC, and IF analysis along with statistical analysis suggest that BGNP-coated SEMS-mediated local heating (50 and 65 °C) inducing the expression of anti-inflammatory HSP70 effectively suppresses tissue hyperplasia after the stent placement in the esophagus. Although further preclinical studies are needed to investigate the efficacy and safety of localized heat treatment, the developed nanofunctionalized SEMS and local heating should be promising for the clinical prevention and treatment of tissue hyperplasia secondary to stent placement in the esophagus and valuable for further various combinational therapies using immune responses.[29]

EXPERIMENTAL SECTION

Materials.

Dopamine hydrochloride, hydrogen tetrachloroaurate-(III) trihydrate ($HAuCl_4$, 99.9%), silver nitrate ($AgNO_3$, 99%), L-ascorbic acid (≥98%), sodium borohydrate (98%), and sodium deoxycholate (≥97%) were used as purchased from Sigma–Aldrich (St. Louis, MO).

Fabrication of BGNP-Coated SEMS.

The cationic polymer was coated on the surface of SEMS through PDA coating prior to deposition of BGNPs on the surface. Dopamine hydrochloride (1 mg/mL) was dissolved in 15 mL of 5 mM Tris buffer (pH 8.5) to form a solution in which the stent was then immersed. The coating process was carried out at room temperature with magnetic stirring for 12 h. The stent coated with PDA was washed with Milli-Q water, and the PDA coating process was repeated two additional times under the same conditions. Next, to adsorb gold ions to the PDA-coated stent, the PDA-coated SEMS was immersed in 5 mM $HAuCl_4$ solution at room temperature for 6 h. Then, the gold-absorbed stent was washed with diluted water. Next, the gold-absorbed stent was immersed in 15 mL of 0.5 mM sodium deoxycholate solution. Then, 0.6 mL of 5 mM $HAuCl_4$ and 0.09 mL of 10 mM $AgNO_3$ solutions were subsequently added. Finally, 0.96 mL of 100 mM of L-ascorbic acid solution was added while stirring; the solution color changed from pale yellow to navy, indicating the formation of BGNPs. After 12 h of reaction, the BGNP-coated stent was washed three times with ethanol and Milli-Q water.

Characterization of BGNP-Coated SEMS.

The surface characteristics of control (bare SEMS), PDA-coated, and BGNP-coated SEMSs were examined by scanning electron microscopy (SEM, JSM-820, JEOL Ltd., Tokyo, Japan) with energy-dispersive X-ray spectroscopy (EDS, INCAx-sight, Oxford Instruments, Abingdon, Oxfordshire, UK). The three SEMSs were fixed on an aluminum pin stub mount using carbon tape, and then the surface of the SEMS was analyzed for the elemental mapping of gold. To analyze the morphology of the BGNP on the surface of SEMS, the coating layer on the stent was peeled off using a razor blade and then washed three times

with water and ethanol through centrifugation. Finally, the shape of the BGNP was observed through TEM (FEI Tecnai Spirit G2, Hillsboro, OR). The ultraviolet–visible (UV–vis) absorption spectra of BGNP were measured by a UV–vis spectrophotometer (Molecular Devices Corp., Sunnyvale, CA, US).

BGNP-Coated SEMS-Mediated Local Heating Properties.

Control (bare SEMS), PDA-coated, and BGNP-coated SEMSs were irradiated with a 1 mm diameter fiber-coupled NIR (808 nm) diode-laser (OCLA LASER, NDLUX Inc., Anyang, Korea) at 1.27 W/cm^2 to investigate PT characteristics in vitro. BGNP-coated SEMSs were irradiated with four different laser powers (0.64, 1.27, 1.91, and 2.55 W/cm^2). BGNP-coated SEMS was irradiated with five repeated NIR irradiations at 1.91 W/cm^2. The temperature increases and thermal images of the stent were examined by using an IR thermal camera (ICI9320P, Infrared Cameras Inc., Beaumont, TX). The images, including temperature data, were stored as electronic image files every 10 s for 5 min. The irradiation was applied for 4 min, and temperatures were recorded for an additional 1 min after removing the irradiation. All in vitro studies were repeated five times to determine statistical reproducibility.

BGNP-Coated SEMS-Mediated Local Heating Properties in Rat Esophagus.

Surgical exploration of the esophagus and stomach of five male Sprague–Dawley rats was followed by gross examination to evaluate the PT effect and determine possible esophageal mucosal changes after NIR laser irradiation at 1.91 W/cm^2 to investigate PT characteristics ex vivo. A BGNP-coated SEMS was placed into the middle portion of the esophagus. Thermal images and temperature changes were obtained at the proximal and distal ends of the stent. Irradiation was applied for 4 min, and temperatures were recorded for an additional 1 min after removing the irradiation.

Animal Studies.

This study was approved by the committee for animal research at our institution and conformed to the Guide for the Care and Use of Laboratory Animals. All rats were supplied with food and water ad libitum and were maintained at 22 ± 2 °C. The body weights of the rats were measured weekly until euthanasia.

Animal Study Design.

For this study, 52 male Sprague–Dawley rats weighing 300–350 g at 9 weeks of age were used. Rats underwent BGNP-coated SEMS placement and were randomly divided into four groups using computer-generated random numbers as follows: Group A (n = 13) received control treatment. Groups B (n = 13), C (n = 13), and D (n = 13) received local heating after stent placement at 50, 65, and 80 °C, respectively. The number of animals was calculated according to a previously published study.[6] Ten rats from each group were euthanized by administrating inhalable pure carbon dioxide at 4 weeks after stent placement for histopathological examination. Additionally, 3 rats from each group were euthanized for Western blot analysis at 3 days after local heating.

Esophageal Stent Placement.

Animals were anesthetized with intramuscular injection of a mixture of 50 mg/kg zolazepam, 50 mg/kg tiletamine (Zoletil 50; Virbac, Carros, France), and 10 mg/kg xylazine (Rompun; Bayer HealthCare, Leverkusen, Germany). A 0.014 in. guidewire (Transcend; Boston Scientific, Watertown, MA) was inserted through the mouth and negotiated into the stomach under fluoroscopic guidance. A customized 6-Fr sheath and dilator were advanced over the guidewire into the lower esophagus. With the sheath left in place, the dilator and the guidewire were removed. A compressed stent was loaded in the sheath and placed in the esophagus using a pusher catheter. The stent was deployed at the level of the midthoracic esophagus under continuous fluoroscopic monitoring. After the procedure, esophagography was performed to verify the position and patency of the stent.

In Vivo BGNP-Coated SEMS-Mediated Local Heating and Endoscopic Examination.

PT-mediated local heating was performed 10 days after stent placement in all rats. For NIR laser irradiation during the in vivo fluoroscope-guided procedure, a 1 mm diameter optical fiber was inserted into a 6-Fr sheath with a radiopaque tip to allow visualization under fluoroscopy. Using fluoroscopic guidance, the sheath and optical fiber were advanced through the mouth into the middle portion of the stented esophagus. NIR laser irradiation was applied for 60 s in all rats. After the procedure, endoscopic examination was performed to identify any tissue changes adjacent to the stent mesh framework using a Hopkins II rigid endoscope (Karl Storz, Goleta, CA). In vivo endoscopic images were also obtained before euthanasia for all rats.

Western Blot Analysis.

To confirm that PT-mediated local heating of the BGNP-coated SEMS resulted in actual tissue heating, HSP70 quantification was performed. Three days after local heating, 3 rats in each group were euthanized and the stent-containing esophageal segments were harvested. Three age-matched healthy male Sprague–Dawley rats maintained under the same conditions were used to determine the normal values of the esophagus. The HSP70 (1:1000; Abcam, Cambridge, UK) antibody was used to evaluate the dose-dependency of HSP70 expression. The membranes were incubated with secondary antibodies (1:10 000; Jackson ImmunoResearch Laboratories, West Grove, PA) conjugated to horseradish peroxidase. Target proteins were detected using ECL Western blotting detection reagents (Amersham Biosciences, Little Chalfont, UK), and antigen–antibody complexes were visualized using Ez-Capture MG software (ATTO Corporation, Tokyo, Japan). CS analyzer software (ATTO Corporation) was used to quantify the bands, and the data are expressed as the ratio of band intensity to that of β-actin.

Histological Examination.

Surgical exploration of the esophagus and stomach was followed by gross examination to determine possible esophageal injury after stent placement or irradiation. The stented esophageal segment was sectioned transversely at the proximal, middle, and distal regions for histological, IHC, and IF analysis to qualitatively and quantitatively assess the degree of granulation tissue formation. Tissue samples were fixed in 10% neutral buffered formalin for

24 h, which was then embedded in paraffin and sectioned. The slides were stained with H&E and MT. Histological evaluation using H&E staining was performed to assess the degree of submucosal inflammatory cell infiltration, number of epithelial layers, thickness of submucosal fibrosis, and granulation tissue-related percentage of the esophageal cross-sectional area of stenosis calculated as 100 × (1 − [stenotic stented area/original stented area]). The degree of inflammatory cell infiltration was subjectively determined according to the distribution and density of the inflammatory cells (graded as 1, mild; 2, mild to moderate; 3, moderate; 4, moderate to severe; and 5, severe). The average values of the number of epithelial layers, thickness of submucosal fibrosis, and degree of inflammatory cell infiltration were represented as the average value of eight points around the circumference.[6] The degree of collagen deposition and percentage of connective tissue area were determined using MT-stained sections. The connective tissue (collagen) area was calculated as follows: 100 × (1 − [connective area/original area]). The extent of collagen deposition was subjectively determined, where 1 = mild, 2 = mild to moderate, 3 = moderate, 4 = moderate to severe, and 5 = severe. Histological analysis of the esophagus was performed using a BX51 microscope (Olympus, Tokyo, Japan). Image-Pro Plus software (Media Cybernetics, Silver Spring, MD) was used for measurements. Histological findings were evaluated based on the consensus of three observers blinded to the group assignments.

Immunohistochemistry.

IHC was performed on paraffin-embedded sections with αSMA (1:200; Abcam), TUNEL (ApopTag, Qbiogene, Darmstadt, Germany), and HSP70 (1:200; Abcam) as the primary antibodies. The sections were visualized with a BenchMark XT IHC automated immunohistochemical stainer (Ventana Medical Systems, Tucson, AZ). The αSMA-, HSP70-, and TUNEL-positive-deposition degrees were subjectively determined, where 1 = mild, 2 = mild to moderate, 3 = moderate, 4 = moderate to severe, and 5 = severe. IHC findings were obtained based on the consensus of three observers blinded to the study.

Immunofluorescence.

The stented esophagus was harvested and fixed by immersion in 4% paraformaldehyde containing perfusion fixative (Electron Microscopy Sciences, Hatfield, PA) at 4 °C, followed by sequential incubation in 15% and 30% sucrose solutions. The fixed samples were embedded in optimal cutting temperature compound, and 6 μm cryostat sections were prepared and collected on slides for subsequent staining. IF staining was performed with Ki67 (1:250; Abcam) and BrdU (1:250; Abcam) antibodies overnight at 4 °C followed by washing with phosphate-buffered saline containing 0.1% Tween 20. After washing, secondary antibody staining was performed using Alexa Fluor 488, Alexa Fluor 594, and 4′-6-diamidino-2-phenylindole (Invitrogen, Carlsbad, CA). Slides were then incubated for 1 h at room temperature. Digital images were collected using a Pannoramic Super-Resolution Confocal microscopy system (3D Histech, Budapest, Hungary).

Statistical Analysis.

Differences between groups were analyzed using the Kruskal–Wallis or Mann–Whitney U test, as appropriate. A p-value of <0.05 was considered statistically significant. Statistical analyses were performed using SPSS software (version 23.0; SPSS, Inc., Chicago, IL).

Supplementary Material

Refer to Web version on PubMed Central for supplementary material.

ACKNOWLEDGMENTS

This research was supported by the Basic Science Research Program (2016R1D1A1A02937042 and 2017R1A2B3011121) through the National Research Foundation of Korea (NRF) funded by the Ministry of Science and ICT (MSIT), Republic of Korea, and by the R21CA173491, R21CA185274, and R21EB017986 grants from the National Cancer Institute and National Institute of Biomedical Imaging and Bioengineering, USA.

ABBREVIATIONS

αSMA	alpha-smooth muscle actin
BGNP	branched gold nanoparticle
DW	deionized water
H&E	hematoxylin and eosin
HSP	heat-shock protein
IHC	immunohistochemistry
IF	immunofluorescence

REFERENCES

(1). Knyrim K; Wagner H-J; Bethge N; Keymling M; Vakil N A Controlled Trial of an Expansile Metal Stent for Palliation of Esophageal Obstruction Due To Inoperable Cancer. N. Engl. J. Med 1993, 329, 1302–1307. [PubMed: 7692297]

(2). Sharma P; Kozarek R Role of Esophageal Stents in Benign and Malignant Diseases. Am. J. Gastroenterol 2010, 105, 258–273. [PubMed: 20029413]

(3). Song H-Y; Jung H-Y; Park S-I; Kim S-B; Lee DH; Kang S-G; Il Min Y Covered Retrievable Expandable Nitinol Stents in Patients with Benign Esophageal Strictures: Initial Experience. Radiology 2000, 217, 551–557. [PubMed: 11058659]

(4). Kim JH; Song H-Y; Choi EK; Kim KR; Shin JH; Lim J-O Temporary Metallic Stent Placement in the Treatment of Refractory Benign Esophageal Strictures: Results and Factors Associated with Outcome in 55 Patients. Eur. Radiol 2009, 19, 384–390. [PubMed: 18726598]

(5). Song H-Y; Park S-I; Do Y-S; Yoon HK; Sung K-B; Sohn K-H; Min Y-I Expandable Metallic Stent Placement in Patients with Benign Esophageal Strictures: Results of Long-term Follow-up. Radiology 1997, 203, 131–136. [PubMed: 9122381]

(6). Jun EJ; Park J-H; Tsauo J; Yang S-G; Kim D-K; Kim KY; Kim MT; Yoon S-H; Lim YJ; Song H-Y EW-7197, An Activin-like Kinase 5 Inhibitor, Suppresses Granulation Tissue after Stent Placement in Rat Esophagus. Gastrointest. Endosc 2017, 86, 219–228. [PubMed: 28137596]

(7). Zhu Y; Cui W; Cheng Y; Chang J; Chen N; Yan L; Li M Biodegradable Rapamycin-eluting Nano-fiber Membrane-covered Metal Stent Placement to Reduce Fibroblast Proliferation in Experimental Stricture in a Canine Model. Endoscopy 2013, 45, 458–468. [PubMed: 23580413]

(8). Baron TH; Burgart LJ; Pochron NL An Internally Covered (lined) Self-expanding Metal Esophageal Stent: Tissue Response in a Porcine Model. Gastrointest. Endosc 2006, 64, 263–267. [PubMed: 16860080]

(9). Jeon S; Eun S; Shim C; Ryu C; Kim J; Cho J; Lee J; Lee M; Jin S Effect of Drug-eluting Metal Stents in Benign Esophageal Stricture: An in vivo Animal Study. Endoscopy 2009, 41, 449–456. [PubMed: 19418400]

(10). Kim E-Y; Song H-Y; Kim JH; Fan Y; Park S; Kim D-K; Lee EW; Na HK IN-1233–eluting Covered Metallic Stent to Prevent Hyperplasia: Experimental Study in a Rabbit Esophageal Model. Radiology 2013, 267, 396–404. [PubMed: 23315658]

(11). Chu KF; Dupuy DE Thermal Ablation of Tumours: Biological Mechanisms and Advances in Therapy. Nat. Rev. Cancer 2014, 14, 199–208. [PubMed: 24561446]

(12). Landsberg R; DeRowe A; Katzir A; Shtabsky A; Fliss DM; Gil Z Laser-induced Hyperthermia for Treatment of Granulation Tissue Growth in Rats. Otolaryngol.–Head Neck Surg 2009, 140, 480–486. [PubMed: 19328334]

(13). Brasselet C; Durand E; Addad F; Vitry F; Chatellier G; Demerens C; Lemitre M; Garnotel R; Urbain D; Bruneval P; et al. Effect of Local Heating on Restenosis and In-stent Neointimal Hyperplasia in the Atherosclerotic Rabbit Model: A Dose-ranging Study. Eur. Heart J 2008, 29, 402–412. [PubMed: 18212388]

(14). Shiina S; Teratani T; Obi S; Sato S; Tateishi R; Fujishima T; Ishikawa T; Koike Y; Yoshida H; Kawabe T; et al. A Randomized Controlled Trial of Radiofrequency Ablation with Ethanol Injection for Small Hepatocellular Carcinoma. Gastroenterology 2005, 129, 122–130. [PubMed: 16012942]

(15). Huber P; Pfisterer P In Vitro and In Vivo Transfection of Plasmid DNA in the Dunning Prostate Tumor R3327-AT1 is Enhanced by Focused Ultrasound. Gene Ther. 2000, 7, 1516–1525. [PubMed: 11001372]

(16). Huang X; El-Sayed IH; Qian W; El-Sayed MA Cancer Cell Imaging and Photothermal Therapy in the Near-infrared Region by Using Gold Nanorods. J. Am. Chem. Soc 2006, 128, 2115–2120. [PubMed: 16464114]

(17). Cai W; Gao T; Hong H; Sun J Applications of Gold Nanoparticles in Cancer Nanotechnology. Nanotechnol., Sci. Appl 2008, 1, 17–32. [PubMed: 24198458]

(18). Ferrari M Cancer Nanotechnology: Opportunities and Challenges. Nat. Rev. Cancer 2005, 5, 161–171. [PubMed: 15738981]

(19). Hirsch LR; Stafford RJ; Bankson J; Sershen SR; Rivera B; Price R; Hazle JD; Halas NJ; West JL Nanoshell-mediated Near-infrared Thermal Therapy of Tumors under Magnetic Resonance Guidance. Proc. Natl. Acad. Sci. U. S. A 2003, 100, 13549–13554. [PubMed: 14597719]

(20). Li L; Wang R; Shi HH; Xie L; Li JDS; Kong WC; Tang JT; Ke DN; Zhao LY In Vitro Study on the Feasibility of Magnetic Stent Hyperthermia for the Treatment of Cardiovascular Restenosis. Exp. Ther. Med 2013, 6, 347–354. [PubMed: 24137187]

(21). Kim D-H; Larson AC Deoxycholate Bile Acid Directed Synthesis of Branched Au Nanostructures for Near Infrared Photothermal Ablation. Biomaterials 2015, 56, 154–164. [PubMed: 25934288]

(22). Zhao K; Cho S; Procissi D; Larson AC; Kim DH Noninvasive Monitoring of Branched Au Nanoparticle-mediated Photothermal Ablation. J. Biomed. Mater. Res., Part B 2017, 105, 2352–2359.

(23). Lee S; Hwang G; Kim TH; Kwon SJ; Kim JU; Koh K; Park B; Hong H; Yu KJ; Chae H; et al. On-Demand Drug Release from Gold Nanoturf for a Thermo-& Chemo-Therapeutic Esophageal Stent (TES). ACS Nano 2018, 12, 6756–6766. [PubMed: 29878749]

(24). Kim E-Y; Shin JH; Jung YY; Shin D-H; Song H-Y A Rat Esophageal Model to Investigate Stent-induced Tissue Hyperplasia. J. Vasc. Interv. Radiol 2010, 21, 1287–1291. [PubMed: 20656225]

(25). Buchner J Supervising the Fold: Functional Principles of Molecular Chaperones. FASEB J. 1996, 10, 10–19. [PubMed: 8566529]

(26). Li J; Chen J; Kirsner R Pathophysiology of Acute Wound Healing. Clin. Dermatol 2007, 25, 9–18. [PubMed: 17276196]

(27). Kim C.-s.; Song H-Y; Jeong IG; Yeo HJ; Kim E-Y; Park J-H; Yoon CJ; Paick SH; Park SW; Bae J-I; et al. Temporary Placement of Covered Retrievable Expandable Nitinol Stents with Barbs in High-risk Surgical Patients with Benign Prostatic Hyperplasia: Work in Progress. J. Vasc. Interv. Radiol 2011, 22, 1420–1426. [PubMed: 21840225]

(28). Song H-Y; Shim TS; Kang S-G; Jung G-S; Lee DY; Kim T-H; Park S; Ahn YM; Kim WS Tracheobronchial Strictures: Treatment with a Polyurethane-covered Retrievable Expandable Nitinol Stent-initial Experience. Radiology 1999, 213, 905–912. [PubMed: 10580974]

(29). Nam J; Son S; Ochyl LJ; Kuai R; Schwendeman A; Moon JJ Chemo-photothermal Therapy Combination Elicits Anti-tumor Immunity Against Advanced Metastatic Cancer. Nat. Commun 2018, 9, 1074. [PubMed: 29540781]

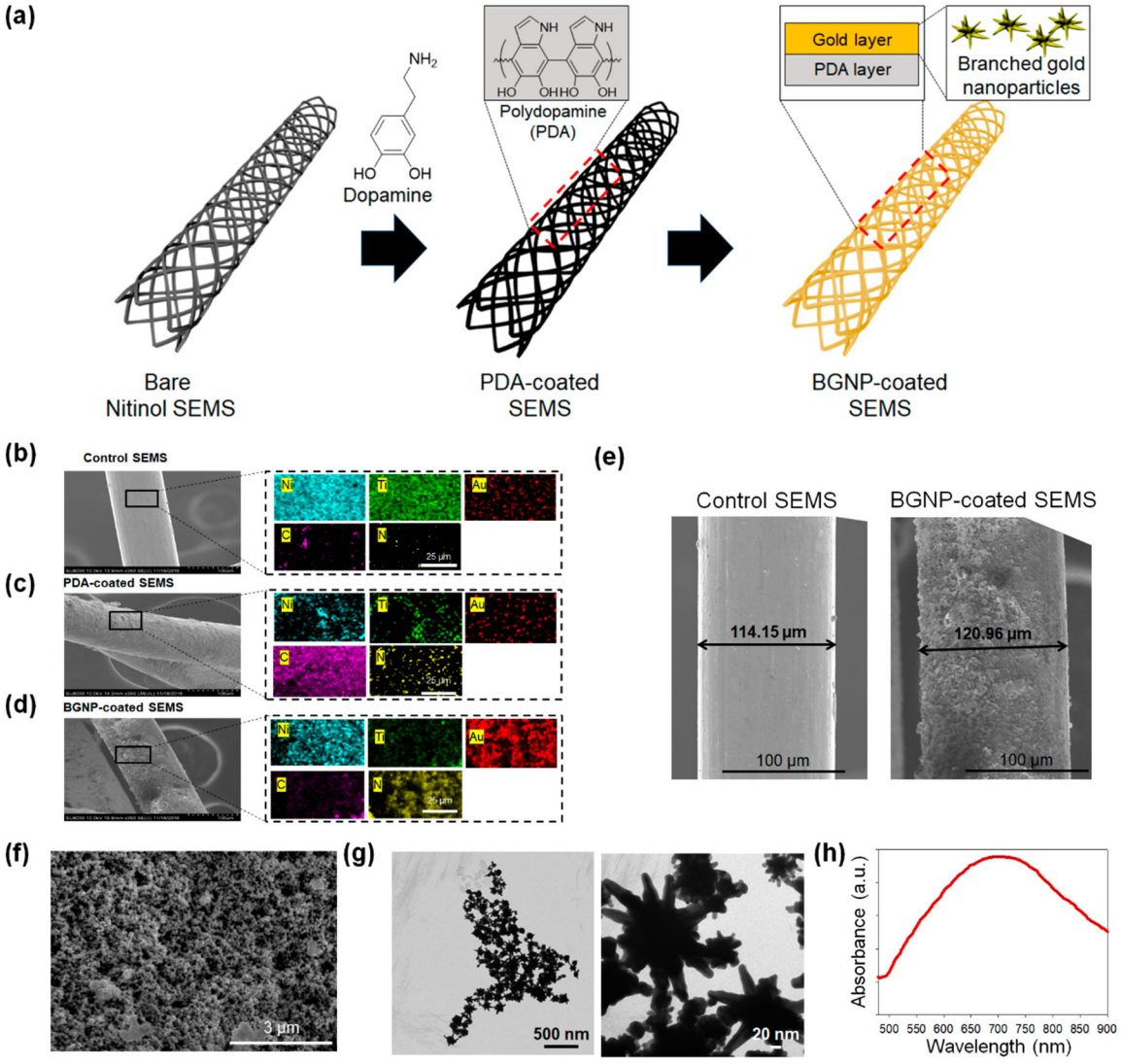

Figure 1.

(a) Schematic illustration of the preparation process for branched gold nanoparticles (BGNP)-coated self-expandable metallic stents (SEMS). The cationic polymer was coated on the surface of SEMS through polydopamine (PDA) coating, and BGNPs were sequentially deposited on the polymer layer. Scanning electron microscopy (SEM) and energy-dispersive X-ray spectroscopy (EDS) mapping analysis of (b) bare SEMS, (c) PDA-coated SEMS, and (d) BGNP-coated SEMS (blue, green, red, pink, and yellow indicate nitinol, titanium, gold, carbon, and nitrogen, respectively). (e) SEM image of bare SEMS and BGNP-coated SEMS. SEM images were analyzed by ImageJ software (U.S. National Institutes of Health, Bethesda, MD) to measure the coating thickness. (f) High-magnification SEM image of the surface of BGNP-coated SEMS. (g) Transmission electron microscopy (TEM) image and (h) UV–vis absorption spectra of BGNP extracted from the surface of BGNP-coated SEMS.

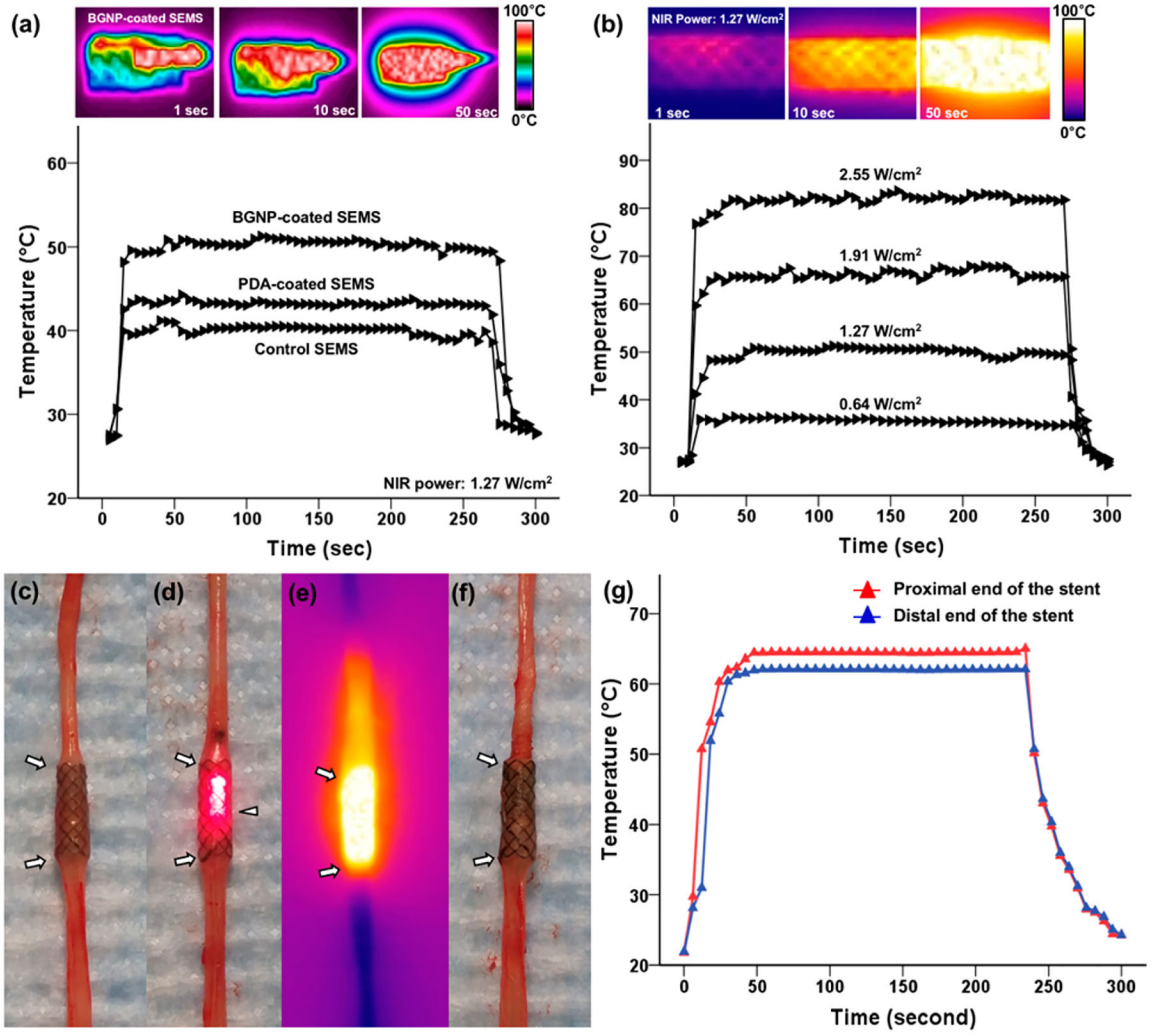

Figure 2.

Infrared thermal camera images and temperature change measurement of (a) bare self-expandable metallic stents (SEMS), polydopamine (PDA)-coated SEMS, and branched gold nanoparticles (BGNP)-coated SEMS under irradiation with an 808 nm laser at 1.27 W/cm^2 and (b) BGNP-coated SEMS under irradiation at four different laser powers (0.64, 1.27, 1.91, and 2.55 W/cm^2). Photographs and a photothermal image of the rat esophagus with a BGNP-coated stent (arrows) (c) before, (d, e) during, and (f) after NIR laser irradiation using an optical fiber (arrowhead, d). (g) Graph showing temperature changes at the proximal and distal ends of the stent under NIR laser irradiation at 1.91 W/cm^2.

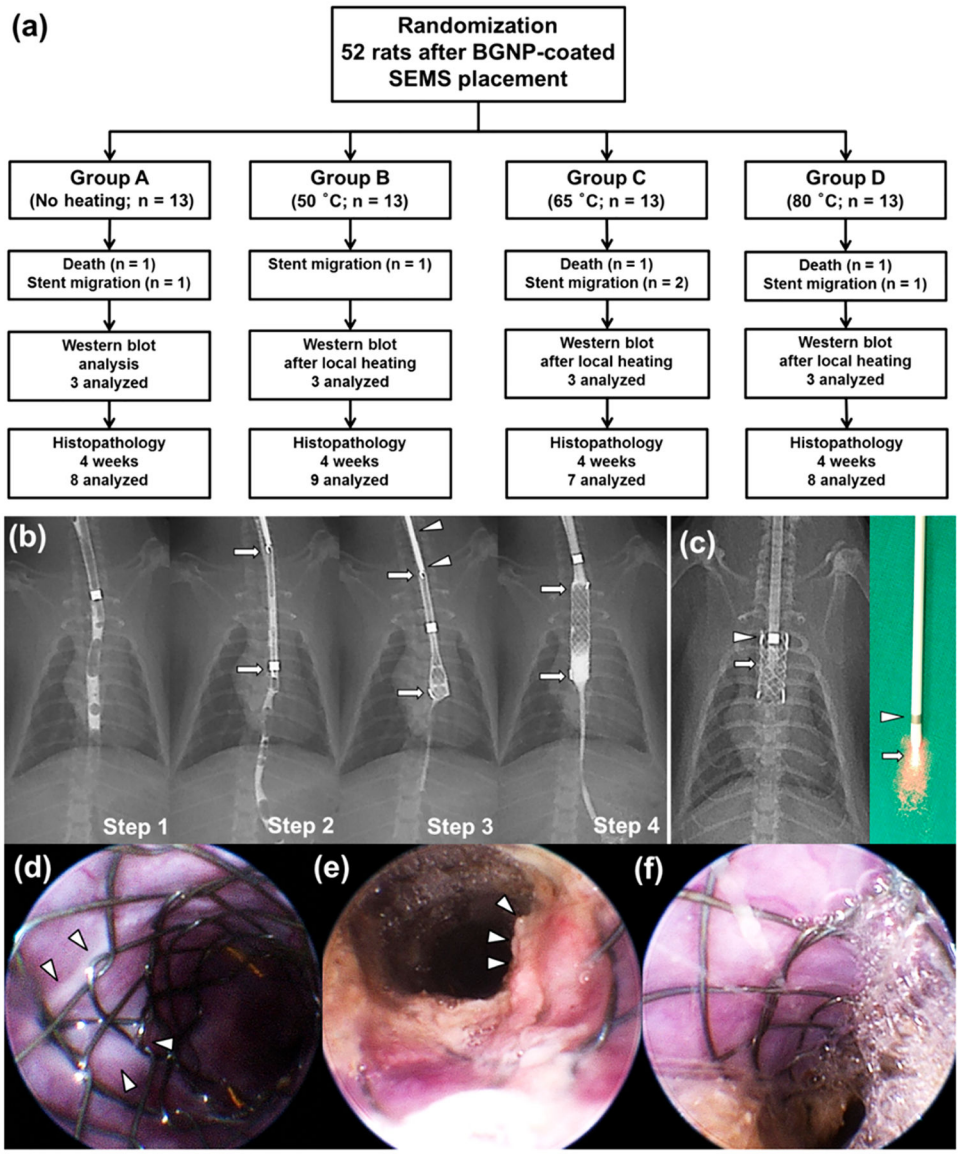

Figure 3.

(a) Flow diagram and study design showing the randomization process and follow up. (b) Radiographic images showing the technical steps of stent placement in a rat esophageal model. Step 1, preprocedural esophagography was performed to determine the location of stent placement in the esophagus; step 2, radiograph showing a compressed stent in a 6-Fr sheath (arrows); step 3, the compressed stent (arrows) was loaded in the sheath and placed using a pusher catheter (arrowheads); step 4, postprocedural esophagography was performed immediately to verify the position and patency of the stent (arrows). (c) Radiographic and digital images of the fiber optic NIR probe advanced through the mouth into the middle portion of the stented esophagus. In vivo endoscopic image obtained (d) immediately after local heating in group B showing white tissue changes (arrowheads) around the stent wire. (e) Endoscopic image obtained 4 weeks after stent placement in group A showing relatively severe tissue hyperplasia through the wire mesh (arrowheads) compared to (f) group B.

(a)

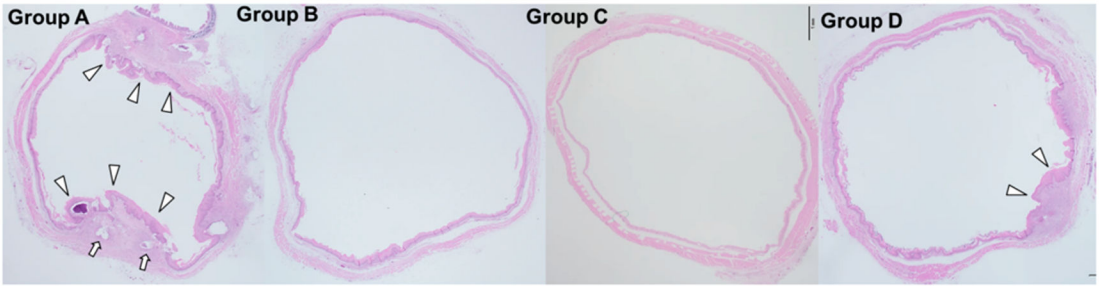

(b)

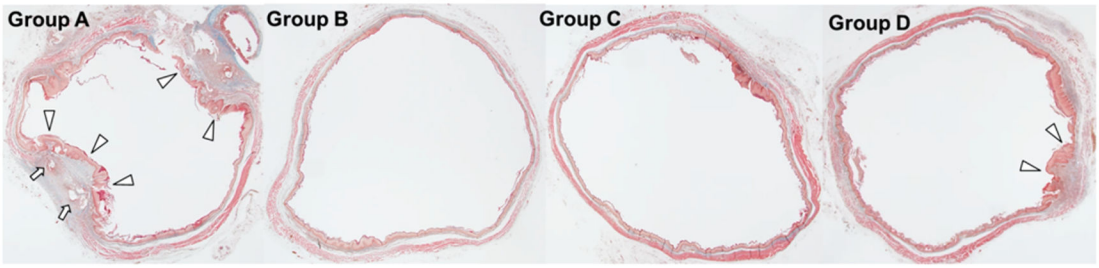

(c)

	Group A	Group B	Group C	Group D	* *p*-value	* *p*-value (A vs. B)	* *p*-value (A vs. C)	* *p*-value (A vs. D)	* *p*-value (B vs. C)	* *p*-value (B vs. D)	* P-value (C vs. D)
Granulation-tissue-area percentage (%)	49.26 ± 7.05	25.82 ± 6.99	27.59 ± 6.63	31.13 ± 7.05	< 0.001	< 0.001	< 0.001	< 0.001	0.567	0.108	0.264
Epithelial-layer number	5.43 ± 0.85	2.71 ± 0.72	3.07 ± 0.73	3.71 ± 0.91	< 0.001	< 0.001	< 0.001	< 0.001	0.197	0.005	0.040
Submucosal-fibrosis thickness (mm)	0.67 ± 0.12	0.29 ± 0.10	0.32 ± 0.15	0.35 ± 0.13	< 0.001	< 0.001	< 0.001	< 0.001	0.707	0.338	0.470
Inflammatory-cell-infiltration degree	2.43 ± 0.76	1.32 ± 0.54	1.21 ± 0.620	2.41 ± 0.64	< 0.001	< 0.001	< 0.001	0.465	-0.597	< 0.001	< 0.001
Connective-tissue-area percentage (%)	31.55 ± 8.33	13.67 ± 3.27	13.92 ± 4.44	15.18 ± 4.12	< 0.001	< 0.001	< 0.001	< 0.001	0.870	0.224	0.341
Collagen-deposition degree	4.08 ± 0.76	2.15 ± 0.69	1.92 ± 0.76	2.23 ± 0.93	< 0.001	< 0.001	< 0.001	< 0.001	0.418	0.869	0.399

Figure 4.

Representative microscopic images of histological sections obtained 4 weeks after stent placement. (a) Hematoxylin and eosin and (b) Masson's trichrome staining of groups A, B, C, and D. Arrows, stent struts; arrowheads, stent-induced granulation tissue (magnification ×1.25). (c) Table of the histological findings of each group. Note: Data are presented as mean ± standard deviation. (*Kruskal–Wallis test. $^{+}$Mann–Whitney U test.)

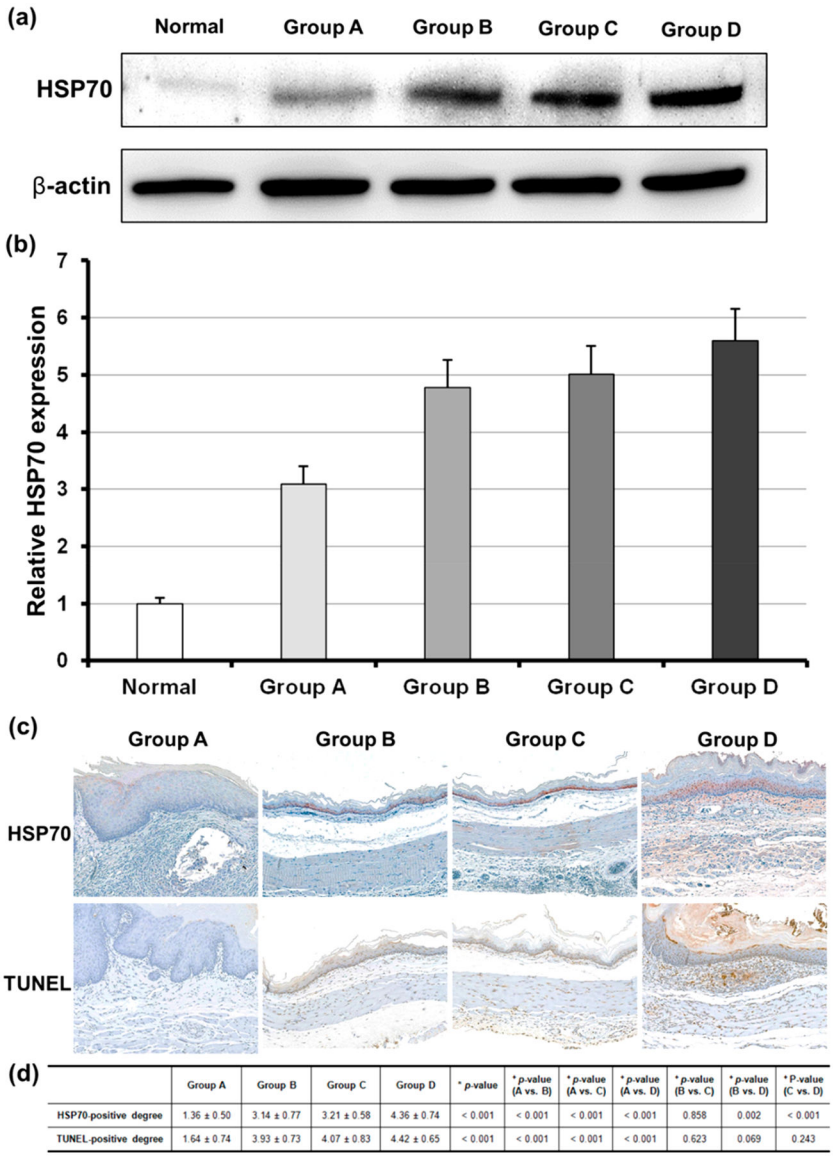

(d)

	Group A	Group B	Group C	Group D	*p-value	*p-value (A vs. B)	*p-value (A vs. C)	*p-value (A vs. D)	*p-value (B vs. C)	*p-value (B vs. D)	*P-value (C vs. D)
HSP70-positive degree	1.36 ± 0.50	3.14 ± 0.77	3.21 ± 0.58	4.36 ± 0.74	< 0.001	< 0.001	< 0.001	< 0.001	0.858	0.002	< 0.001
TUNEL-positive degree	1.64 ± 0.74	3.93 ± 0.73	4.07 ± 0.83	4.42 ± 0.65	< 0.001	< 0.001	< 0.001	< 0.001	0.623	0.069	0.243

Figure 5.

(a and b) Relative heat shock protein 70 (HSP70) expression after local heating gradually increased in a heating dose-dependent manner. (c) Representative microscopic images of immunohistochemistry sections obtained 4 weeks after stent placement in each group. HSP70 and TUNEL expression was significantly increased in the heated groups compared to in the control group (magnification ×20). (d) Table of the immunohistochemistry findings of each group. Note: Data are presented as mean ± standard deviation. (*Kruskal–Wallis test. $^{+}$Mann–Whitney U test.

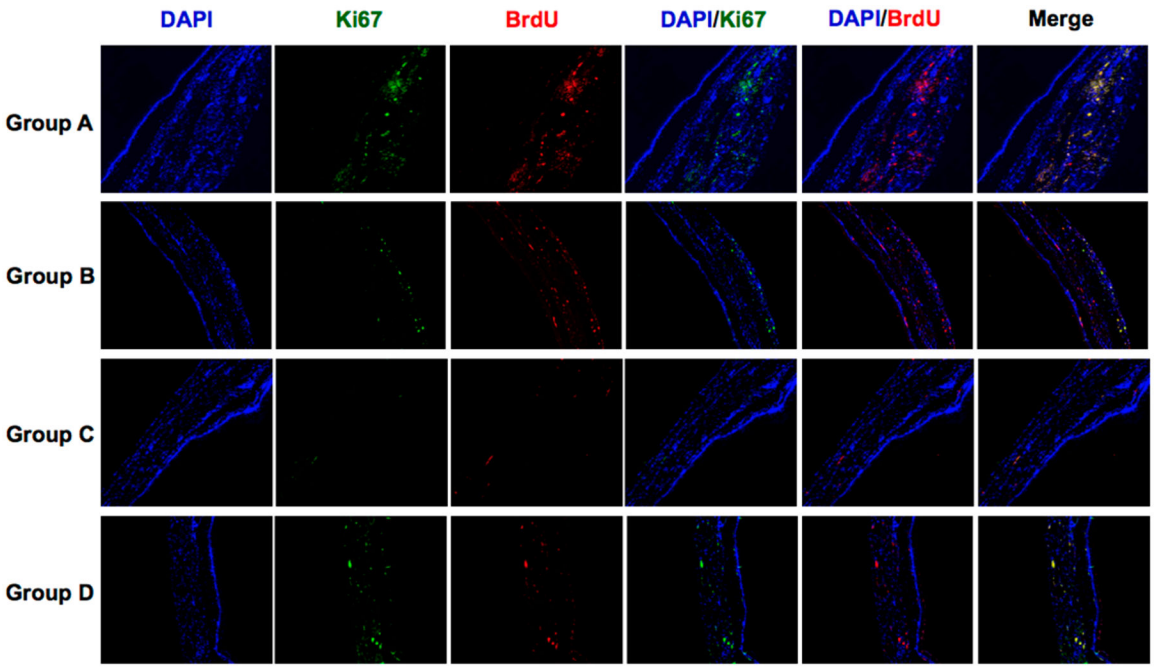

Figure 6.

Representative Ki67 and BradU immunofluorescence images showing that BGNP-coated SEMS-mediated local heating suppressed cell proliferation/mitosis (magnification ×40).